Exploring the association of *Fermi* sources with Young Stellar Objects

P. Munar-Adrover[1], J.M. Paredes[1], G.E. Romero[2], R. Walter[3]

[1] Departament d'Astronomia i Meteorologia and ICCUB, Universitat de Barcelona (IEEC-UB). *Email: pmunar@am-ub.es*
[2] Instituto Argentino de Radioastronomía (CCT La Plata, CONICET)
[3] *INTEGRAL* Science Data Centre

Abstract

Massive protostars have associated bipolar outflows which can produce strong shocks when interact with the surrounding medium. In these conditions particle acceleration at relativistic velocities can occur leading to gamma ray emission, as some theoretical models predict. To identify young stellar objects (YSO) that may emit gamma rays we have crossed the *Fermi* First Year Catalog with some catalogs of known YSOs, and we have conducted Montecarlo simulations to find the probability of chance coincidence. With this crossing we obtained a list of YSOs spatially coincident with *Fermi* sources that may show gamma ray emission. Our results indicate that ~70% of the candidates should be γ-ray sources with a confidence of ~5σ. We have studied the coincidences one by one to check the viability of these YSOs as potential counterparts of *Fermi* sources and plan further detailed observations of few of them. We also conducted a stacking analysis of all the available *INTEGRAL* data in order to get better sensitivity. We get an upper limit to the flux

γ-ray production scenario

Massive YSOs show collimated outflows and thermal radiation has been detected up to distances of 10^{16}-10^{18}cm from the central star. These are strongly supersonic jets and in some cases, non-thermal radio lobes have been detected at distances of Z_j~ 1pc (Garay et al. 2003). These radio lobes are probably generated by strong terminal shocks of the jets, which also ionize the shocked material. The possibility of YSOs to be γ-ray emitters has already been discussed in Araudo et al. 2007 and Bosch-Ramon et al. 2010.

Magnetic fields should also be present, since they play an important role in supporting the cloud before the gravitational collapse. Under these conditions, particles can be accelerated up to relativistic energies via diffusive shock (Fermi I) acceleration (e.g. Bell 1978). These particles would produce the non-thermal radiation found in the lobes and could generate significant emission in a broad spectral range, from radio to γ-rays (Bosch-Ramon et al. 2010). We assume, that the non-thermal radio lobes are the regions in which protostellar jets terminate.

The action of the jet head on the external medium leads two shocks (Fig. 1), one moving in the cloud material and one moving in the jet itself: the bow shock and the reverse shock, respectively. The observed non-thermal radio emission would be generated at the shocks where the particles are accelerated.

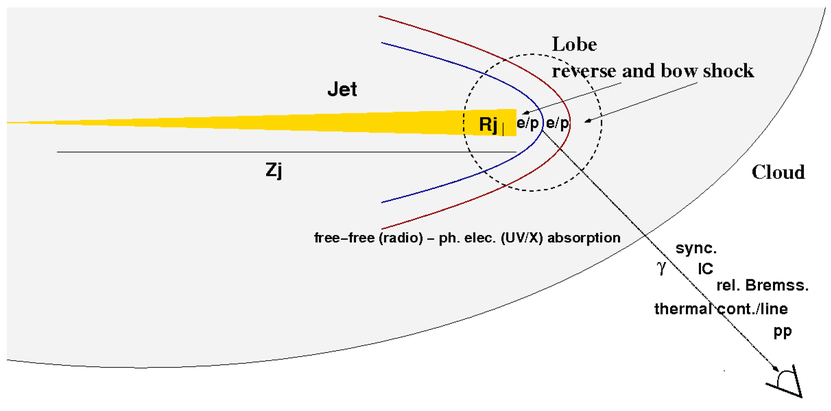

Fig. 1. Diagram of the termination region of the jet of a massive YSO. The two shocks are represented. Particles can be accelerated in these shocks and produce non-thermal radiation via interaction with the surrounding matter, the radiation field and the magnetic field. (Bosch-Ramon et al. 2010)

The First *Fermi-LAT* Catalog (1FGL)

The 1FGL contains 1451 high-energy sources detected in the 100 MeV to 100 GeV range by the Large Area Telescope, the primary science instrument on the *Fermi* Gamma-ray Space Telescope during the 11 months of the science phase of the mission, which began on 2008 August 4 (Abdo et al. 2010). The 1FGL includes source location regions, defined in terms of elliptical fits to the 95% confidence regions, power-law spectral fits and flux measurements in 5 energy bands for each source.

Method

- We have used a computer code that determines the angular distance between two points in the sky, taking into account the positional uncertainties in each of them.
- We ran the code with the 1392 sources of the 1FGL that have not been firmly identified, and the 637 sources identified as YSOs in the RMS survey (J.S. Urquhart et al. 2009).
- We have found 12 γ-ray sources of the 1FGL catalog positionally coincident with YSOs from the RMS Survey. In order to estimate the statistical significance of these coincidences, we have simulated a large number of sets of *Fermi* sources. Specifically, we have simulated 1500 populations of 1392 Fermi sources, through rotations on the celestial sphere, displacing a source with original galactic coordinates (l, b) to a new position (l_0, b_0) (as in Romero et al. 1999).
- The new positions have been obtained doing $l_0 = l+R_1 \times 360^o$, where R_1 is a random number between 0 and 1. In order to retain the histogram of the distribution of sources in galactic latitude we replace $b_0 = b+R_2 \times 1^o$, and then, if the integer part of b_0 is greater than the integer part of b or if the sign of b_0 and b are different, we replace b_0 by $b_0 + 1^o$. Similarly, we have conducted a second simulation, using a 2^o-binning distribution.
- The separation between the *Fermi* source and the YSO is calculated in each case using the statistical parameter R (Allington-Smith et al. 1982)

$$R=\sqrt{\frac{(\Delta\alpha\cos\delta)^2}{\sigma_{i_\alpha}^2+\sigma_{j_\alpha}^2}+\frac{\Delta\delta^2}{\sigma_{i_\delta}^2+\sigma_{j_\delta}^2}}\leqslant 1$$

where $\sigma_{\alpha i}$, $\sigma_{\delta i}$ is the uncertainty in the position of the source, and *i* and *j* are *Fermi* and RMS sources, respectively. The case R=1 means that the RMS source is just on the border of the error ellipse of the Fermi source.

Table 1: Positional coincidence of *Fermi* sources with MYSOs.

Fermi Name (1FGL)	RA (°)	Dec (°)	95% Semi Major Axis (°)	Spectral Index Γ ($F \propto E^{-\Gamma}$)	Flux(E>100 MeV) $\times 10^{-11}$ erg cm^{-2} s^{-1}	MSX Name	RA (°)	Dec (°)	Δθ (°)	Distance* (kpc)	L_{bol}* ($\times 10^3 L_\odot$)
J0541.1+3542	85.2805	35.7091	0.1397	2.41±0.13	1.6±0.5	G173.6328+02.8064	85.27929	+35.82633	0.12	1.6[a]	4.8[d]
						G173.6339+02.8218	85.29592	+35.83380	0.13	1.6[a]	3.2[e]
						G173.6882+02.7222	85.22758	+35.73558	0.05	1.6[a]	–
J0647.3+0031	101.8417	0.5289	0.2150	2.41±0.11	1.9±0.5	G212.0641−00.7395	101.80567	+0.43514	0.10	6.4[b]	25[f]
J1256.9−6337	194.2474	−63.6212	0.1955	2.26±0.12	4.9±1.1	G303.5990−00.6524	194.35546	−63.51650	0.12	11.3[b]	8.3[f]
J1315.0−6235	198.7635	−62.5971	0.1860	2.31±0.12	6.9±0.0	G305.4840+00.2248	198.40016	−62.53708	0.18	3.6[b]	3.8[f]
J1651.5−4602	252.8831	−46.0340	0.2258	2.21±0.07	13.9±3.4	G339.8838−01.2588[1]	253.01942	−46.14267	0.14	2.6[b]	21.0[f]
J1702.4−4147	255.6039	−41.7859	0.0800	2.39±0.07	8.7±2.0	G344.4257+00.0451B	255.53674	−41.78303	0.05	5.0[b]	15.0[f]
						G344.4257+00.0451C	255.53587	−41.78617	0.05	5.0[b]	15.0[f]
J1846.8−0233	281.7001	−2.5628	0.1262	2.21±0.06	9.3±2.3	G030.1981−00.1691	281.76274	−2.51003	0.08	7.4[b]	29.0[f]
J1848.1−0145	282.0470	−1.7605	0.0859	2.23±0.04	9.5±3.2	G030.9726−00.1410	282.09178	−1.80842	0.07	5.7[b]	3.9[f]
						G030.9959−00.0771	282.04516	−1,75808	0.0044	5.7[b]	5.1[f]
J1853.1+0032	283.2884	0.5366	0.5207	2.18±0.07	5.7±1.7	G032.8205−00.3300	282.04436	−1.75703	0.34	5.1[b]	17.0[f]
						G033.3891+00.1989	282.89092	+0.49750	0.40	5.1[b]	11.0[f]
						G033.3933+00.0100	283.06109	+0.41528	0.26	6.8[b]	7.9[e]
						G033.5237+00.0198	283.11179	+0.53569	0.34	6.8[b]	7.9[e]
						G034.0126−00.2832	283.60437	+0.83239	0.43	13.3[b]	34.0[f]
						G034.0500−00.2977	283.63454	+0.85914	0.47	13.3[b]	24.0[f]
J1925.0+1720	291.2748	17.3485	0.1443	2.28±0.12	2.4±1.0	G052.2025+00.7217A	291.24933	+17.42169	0.08	10.2[b]	15.0[f]
						G052.2078+00.6890	291.28553	+17.41317	0.07	10.2[b]	20.0[f]
J1943.4+2340	295.8667	23.6815	0.1118	2.23±0.11	2.6±0.7	G059.7831+00.0648[2,3]	295.79680	+23.73433	0.08	2.2[a]	6.8[f]
J2040.0+4157	310.0154	41.9533	0.1970	2.66±0.06	7.9±1.2	G081.5168+00.1926	309.99066	+41.98739	0.04	1.7[c]	0.704[f]

[1]Detected in radio at 8.6 GHz with integrated flux of 2.6 mJy; [2]Detected in radio at 8.6 GHz with integrated flux of 1.0 mJy. [3]Observed in the X-ray with *Chandra* (Beuther et al. 2002); Distances: [a]distance to the complex, taken from the literature, [b]kinematic distance determined from the systemic velocity of the complex, [c]distance has been taken from the literature. Luminosities: [d]*IRAS* fluxes, [e]*MSX* 21 μm band flux using a scaling relationship determined from a comparison with sources where spectral energy distribution (SED) fits have been possible. [f]SED fit to the available infrared fluxes (*2MASS, MSX, MIPSGAL/IGA*) and literature (sub)millimetre fluxes. *data obtained from http : //www.ast.leeds.ac.uk/cgi – bin/RMS/RMS_DATABASE.cgi.

Object type	Coincident γ-ray sources	Simulated $1^\circ - bin$	Probability $1^\circ - bin$	Simulated $2^\circ - bin$	Probability $2^\circ - bin$
YSO	12	4.4±2.0	1.8×10^{-4}	3.6±1.8	5.6×10^{-6}

Table 2. Statistical results obtained from simulations. Latitude galactic coordinate has been constrained, while galactic longitude remains free

The RMS Survey

MYSOs are luminous ($L > 10^4 L_{Sun}$), embedded infrared sources that still have to begin to ionize their surroundings to form an ultra-compact H II region. They are likely to be already burning hydrogen in their cores, whilst still accreting at the surface. They drive bipolar molecular outflows and often have a compact ionized stellar wind and associated maser activity. Most of their energy comes out in the infrared after reprocessing by the dense circumstellar dust envelope. This is therefore the most logical and unbiased way of searching for such objects.

The Red MSX Source (RMS) survey is an ongoing multi-wavelength observational program with the objective of providing a well-selected sample of MYSOs in the entire Galaxy (Urquhart et al. 2009). They have identified ~2000 MYSO candidates by comparing the colours of MSX and 2MASS point sources with those of well known MYSOs.

The survey also uses high resolution radio continuum observations at 6cm obtained with the VLA in the northern hemisphere, and at 3.6 cm and 6 cm with ATCA in the southern hemisphere, that help to distinguish bitween genuine MYSOs and other types of objects, such as Ultra Compact HII regions, evolved stars or Planetary Nebulae, that contaminate the sample.

In addition to these targeted observations, archival data of previous VLA survey of the inner Galaxy has been used.

This ongoing program has provided a sample of 556 well identified MYSOs up to day, which have been used in our work.

Analysis of *INTEGRAL* data

We looked for nonthermal hard X-ray emission in the public archive of the *INTEGRAL* satelite, analyzing the data corresponding to the Fermi sources we found in coincidence with YSOs. Our results show that none of the Fermi sources was detected by *INTEGRAL*. We also analysed the data corresponding to five YSOs which show non-thermal radio emission, such as IRAS 16547-4247 (Garay et al. 2003), IRAS 18273+0113 (Rodríguez et al. 1989), HH80-81 (Martí et al. 1993, Carrasco-González et al. 2010) and the Turner-Welch source (Reid et al. 1995). The results of the analysis of these five sources are also negative. The model for the source IRAS 16547-4247 (see Bosch-Ramon et al. 2010) predicts a flux in the *INTEGRAL* energy range (17-80 keV) of ~14μCrab units. The upper limits we calculate do not contradict the model predictions but we cannot constrain the model parameters since the upper limits are about two orders of magnitude above the theoretical expectations (~1.5 mCrab for energies between 20-40 keV).

To get a better sensitivity, we perform a stacking analysis of all the available *INTEGRAL* public data corresponding to the positions of all the sources in the RMS Survey catalog of YSOs except those which are closer than 3° to any *INTEGRAL* source, to avoid contamination coming from bright known sources. After this step, we still have 493 YSO positions. In this analysis all the images of the regions with a YSO are superposed and treated as a single observation with a total exposure time equal to the sum of all the exposures. With this method we got a total exposure time of ~10^9 s.
We do not detect signal with this analysis, but we improve the upper limit we got analysing the sources individually. The flux upper limit is $F_{UL(17<E<80keV)} = 16.7 \pm 3.4$ μCrab Units. We also calculate upper limits in narrow energy bands (see Table 3).

Energy range (keV)	Flux UL (μCrab units)
17 – 80	16.7±3.4
17 – 30	15.9±3.1
30 – 40	11.4±2.2
50 – 60	2.1±4.4
80 – 100	58.8±11.8

Table 3. Flux upper limits in μCrab units for different energy bands calculated from the stacking analysis results.

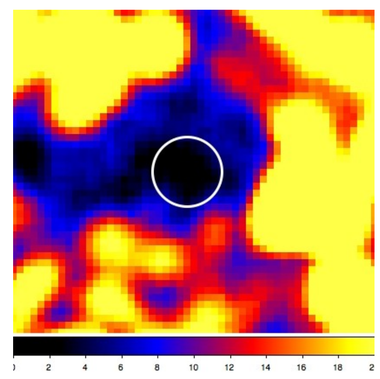

Figure 2. Significance map resulting form the stacking analysis. The white circle marks the position where all the YSOs are stacked toghether. It can be seen that the significance at this position is below 2.

Results

- We find 12 *Fermi* sources being positionally coincident with 22 YSOs (see Table 1). From Table 2 we can see that there is a correlation at 5σ level.

- The probability of a pure chance association is as low as 5.6×10^{-6} for the 2^o-binning simulations (1.8×10^{-4} for the 1^o-binning). The results of this study have been accepted for publication in Astronomy & Astrophysics (Munar-Adrover et al. 2011).

- One of the most interesting coincidences is the one of the *Fermi* source **1FGL J1943.4+2340**. In the radio data from the NVSS that there is a region of massive star formation with many X-ray sources (see Beuther et al. 2002), where the YSO from the RMS survey is located.

- Another interesting case is the one of the *Fermi* source **1FGL J1853.1+0032**. This source has an error circle of more than 0.5^o and thus, we find a large number of sources inside the error ellipse. Some of the sources are the SNR G033.7+0.00, SNR G033.6+0.01 and the pulsar PSR J1852+0040 which, even when the source has no proposed counterpart, are probable candidates to be the responsible of the γ-ray emission.

- Finally, we can comment the case of the *Fermi* source **1FGL 1925.0+1720**. There is a likely extended radio source within the error ellipse of the *Fermi* source, and near the two RMS sources.

- From the literature we find 5 YSOs that show radio no -thermal emission: IRAS 16547-4247, the Turner-Welch source, IRAS 18273+0113 and HH 80-81. The analysis of public *INTEGRAL* data of these sources yields no evidence for a detection. The upper limits for the modeled source IRAS 16547-4247 are in agreement with the model but the parameters cannot be constrained.

- The stacking analysis of *INTEGRAL* data reveals no evidence of signal. The flux upper limit for energies between 17 and 80 keV is 16.7 ±3.4 μCrab units.

References

Abdo A.A. et al., 2010, ApJ Suplement Series, 188, 405-436
Allington-Smith J.R., Perryman M.A.C., Longair M.S. et al., 1982, MNRAS, 201, 331-344
Araudo A.T., Romero G.E., Bosch-Ramon V., and Paredes J.M., 2007, A&A, 476, 1289-1295
Bell A.R., 1978, MNRAS, 182, 147
Beuther H., Kerp J. Preibisch T., Stanke T., Schilke P., 2002, A&A, 395, 169
Carrasco-González C., Rodríguez L.F., Anglada G., et al., 2010, Science, 330, 1209
Bosch-Ramon V., Romero G.E., Araudo A.T. and Paredes J.M., 2010, A&A, 511, A8
Garay G., Brooks K.J., Mardones D., and Norris R.P., 2003, ApJ, 587, 739-747
Lumsden S.L., Horae M.G., Oudmaijer R.D., and Richards D., 2002, MNRAS, 336, 621-636
Martí J., Rodríguez L.F., Reipurth B., 1993, ApJ, 416, 208
Molinari S., Brand J., Cesaroni R. et al., 1998, A&A, 336, 339–351
Munar-Adrover P., Paredes J.M., Romero G.E., 2011, arXiv:1104.2012
Price S.D., Egan M.P., Carey S.J. et al., 2010, AJ, 121, 2819-2842
Reid, M. J.; Argon, A. L.; Masson, C. R., et al. 1995, ApJ, 443, 238R
Rodríguez L.F., Curiel S., Moran J.M., et al. 1989, ApJ, 346, L85
Romero G.E., Benaglia P. and Torres D.F., 1999, A&A, 348, 868-876
Sridharan T.K., Beuther H., Schilke P. et al., 2002, ApJ, 566, 931-944
Urquhart J.S., Horae M.G., Purcell C.R. et al. , 2009, 2009, A&A 501, 539-551